Filling of Solvent Shells about Ions: 1. Thermochemical Criteria and the Effects of Isomeric Clusters

ARTICLE *in* THE JOURNAL OF PHYSICAL CHEMISTRY · DECEMBER 1986

Impact Factor: 2.78 · DOI: 10.1021/j100283a006

cm^{-1}) in TEA (where Chl a·L_1 occurs), despite superior resolution (Figure 3).

The number of extra ligands should evoke some changes in the vibronic structure, since an axial shift of the Mg atom takes place, and the charge is redistributed in the central part of the Chl a molecule as in the case of PChl. Indeed, for the monoligated form the ω_e values of 567, 601, 877, 912, 1004, and 1122 cm^{-1} seem to be characteristic (Figure 3). Alternatively, in the Chl a·L_2 spectra the ω_e of 592 and 616 cm^{-1} arise and the ω_e = 982 peak diminishes (Figure 6). It may be noticed that the respective ω_e values are very close in pyridine, 1-butanol, and methanol–ethanol,[28] while a slightly different set is seen in TEA, ether,[9] DMF, and γ-collidine (spectra not shown). Therefore, the spectral changes are dependent on the Chl a solvation state rather than on a specific host, and the solvates with different Mg coordination number can be distinguished without difficulty in the case of high vibrational resolution by using vibrational frequencies and $S_2 \leftarrow S_0$ band positions.

Conclusions

The influence of the solid host on the spectroscopic properties of the pigment molecule is determined, generally, by three types of interactions: the electron–phonon coupling, the specific solvation, and the nonspecific solvation. We have characterized the first one by relative line-to-background intensity in the narrow-band recorded excitation spectra. The best sharp-line spectra could be obtained in amorphous, vitreous matrices. Snowy, crystalline samples yield poorer vibronic resolution, at least in the case of the Chl a series.

The nature of the molecular complexes of the pigment with matrix molecules depends on the specific properties of the solvent, its nucleophilicity, and its electrophilicity. The extracoordination number (1 or 2) of the PChl and Chl a central Mg atom could be ascertained by using well-resolved excitation spectra.

The nonspecific interaction affects negligibly the Debye–Waller factor and the type of Chl a solvates. However, the width and maximum of the inhomogeneous site-distribution function (as well as absorption and nonselectively excited fluorescence maxima) are related (via dispersion interaction and Stark shift) to the local polarizability and charge density in the closest environment of pigment molecules.

The PChl(ide) and Chl(ide) a molecules bound to the lipoproteins in plant cells are likely to be embedded in a rigid glasslike medium, which favors the observation of vibrationally resolved spectra.[12,13] Undoubtedly, the high-resolution laser spectroscopy will contribute to the understanding of the state of pigments in etiolated and greening plants, subchloroplast particles, etc.

Registry No. TEA, 121-44-8; DMF, 68-12-2; THF, 109-99-9; PChl, 14751-08-7; 4-vinyl-PChl, 22429-66-9; Chl a, 479-61-8; Chl a', 22309-13-3; EtChlide a, 14444-88-3; pryo-Chl a, 21028-91-1; BuOH, 71-36-3; MeOH, 67-56-1; EtOH, 64-17-5; Et_2O, 60-29-7; 1-BuOH, 78-83-1; cyclohexane, 110-82-7; γ-collidine, 108-75-8; pyridine, 110-86-1; dioxane, 123-91-1.

Filling of Solvent Shells about Ions. 1. Thermochemical Criteria and the Effects of Isomeric Clusters

Michael Meot-Ner* (Mautner) and Carlos V. Speller†

Chemical Kinetics Division, Center for Chemical Physics, National Bureau of Standards, Gaithersburg, Maryland 20899 *(Received: April 14, 1986)*

Solvent shells can build up by the stepwise attachment of molecules to gas-phase ions. The filling of a solvent shell by the sth solvent molecule is indicated by a discontinuous drop in the attachment energy at the $(s + 1)$th solvent molecule, i.e., a discontinuous drop in the plots of $\Delta H^\circ_{n-1,n}$ vs. n (enthalpy sequences) after $n = s$. Another indication is a gap in the spacing of consecutive van't Hoff plots after $n = s$. As examples, new series of measurements confirm shell filling in $H_3O^+ \cdot nH_2O$ after $n = 3$ and show an unexpected shell effect in $OH^- \cdot nH_2O$ after $n = 3$. On the other hand, no shell effect, within experimental accuracy, is found in $NH_4^+ \cdot nH_2O$. Thermochemical criteria based on enthalpy sequences and the spacing of consecutive van't Hoff plots are developed quantitatively and applied to data on clustering about metal ions and onium ions. Satisfactory evidence for the distinct filling of shells is found in 14 and tentative evidence is found in another 15 out of 59 systems. The criteria are satisfied for the distinct filling of the first shell in the hydration of H_3O^+ and OH^-, the ammoniation of NH_4^+, and the filling of the second shell in the hydration of H_2COH^+, $(CH_3)_2COH^+$, and several other monoprotonic onium ions. In all cases, a necessary condition for the distinct filling of a shell is that $-\Delta H^\circ_{s-1,s}$ must be larger by at least 3 kcal/mol than the condensation enthalpy of the solvent. Otherwise, neutral-like condensation can commence and the filling of the outer shell may start before the filling of the first shell. Alternatively, the filling of shells may occur in parallel, and isomeric clusters may form. However, numerical calculations show that in typical cases the presence of isomeric clusters may cause only small errors (±1 kcal/mol) in the thermochemical measurements.

Introduction

The clustering of solvent molecules about ions constitutes a process of stepwise ion solvation. Measurement of the thermochemistry of the clustering reaction 1 therefore allows insights into ion–solvent interactions in the inner solvation shells.

$$BH^+ \cdot (n-1)L + L \rightleftarrows BH^+ \cdot nL \qquad (1)$$

The thermochemistry of clustering of a variety of inorganic or organic ligands about metal ions M^+ or protonated molecules BH^+ has been obtained.[1-3] In these studies an equilibrium mixture of the reactants and products is generated in the source of a high-pressure mass spectrometer. The relative equilibrium ratios of $BH^+ \cdot (n-1)L$ and of $BH^+ \cdot nL$ are obtained from the mass spectrometric ion signal intensities. The equilibrium constant is then calculated from eq 2.

$$K = \frac{[BH^+ \cdot nL]}{[BH^+ \cdot (n-1)L]P_L} \qquad (2)$$

The enthalpy and entropy changes of reaction 1 can be obtained from the slopes and intercepts of van't Hoff plots, i.e., plots of

† Present address: Departamento de Fisica, Universidade Federal de Pernambuco, 50.000 Recife, Pernambuco, Brazil.

(1) Kebarle, P. *Annu. Rev. Phys. Chem.* **1977**, *28*, 445.
(2) Keesee, R. G.; Castleman, A. W. *J. Phys. Chem. Ref. Data*, in press.
(3) Meot-Ner (Mautner), M. *J. Am. Chem. Soc.* **1984**, *106*, 1283.

ln K vs. $1/T$. Implicit in this standardly used treatment is that $\Delta H°$ and $\Delta S°$ are constant over the temperature range of the measurement. In the van't Hoff plots obtained to date, no curvatures were observed that would suggest deviation from this assumption. The constancy of $\Delta H°$ and $\Delta S°$ over the experimental temperature range will be therefore assumed in this paper.

The mass spectrometric measurements of the clusters yield no information on the structures of the cluster ions. Usually, structural inferences may be drawn from the thermochemistry, especially when it is coupled with theoretical calculations. Nevertheless, reasonable alternative structures may be drawn for many clusters, and the actual most stable structure is not always obvious.

A question of interest in clustering about ions is whether the solvent builds up about the ion in distinct shells. For example, it may be expected that a certain number of solvent molecules can attach intimately to a core ion, and once no more solvent molecules are sterically permitted about the ion a new solvent shell will start to form. If the attachment energies to the outer shell are substantially smaller than to an inner shell, then a discontinuous drop will occur in plots of $-\Delta H°_{n-1,n}$ after the shell-filling step (denoted here as the sth step). Also, this may require a relatively large drop in temperature, i.e., a large increase in $1/T$, to start building the outer shell, which is observed in a large spacing of the van't Hoff plots after the sth step. These criteria were used qualitatively, mainly by Kebarle and co-workers,[4-9] Castleman and co-workers,[10-12] and Meot-Ner[3] to search for shell-filling effects. In the present paper we shall first illustrate these effects by examining the data for four hydration and ammoniation systems. As we shall note, the thermochemical effects of shell filling tend to be within the experimental error, and replicate sets of data are sometimes contradictory in this respect. Therefore, we shall present new sets of data on three basic systems, the hydration of H_3O^+, NH_4^+, and OH^-. We shall then formulate the thermochemical criteria quantitatively and apply this test to all the available clustering data to see in which cases is there satisfactory evidence for the distinct formation of solvent shells.

Usually, major effects of shell-filling behavior occur only in special cases when the formation of outer shells is clearly blocked. For example, large drops from 30 to 10–15 kcal/mol in $-\Delta H°_{n-1,n}$ occur after $n = 1$ in the clustering of onium ions in which hydrogen bonds to the outer shell are blocked, e.g., in $(Me_2O)_nH^+$ and $(MeCN)_nH^+$, where two molecules complete the inner shell about the proton.

A different situation arises, for example, in the hydration of H_3O^+ or the hydration and ammoniation of NH_4^+ or metal ions. In these clusters several H_2O or NH_3 molecules can directly attach or hydrogen bond to the core ion, and it is possible to attach to this inner shell an infinite network of hydrogen bonded solvent molecules. However, after the attachment of three or four solvent molecules to the core ion, $-\Delta H°_{n-1,n}$ often decreases below 15 kcal/mol, i.e., only a few kcal/mol more than the lower limiting values of 10 ± 1 kcal/mol (i.e., about the enthalpy of condensation of water). At this point hydrogen bonding energies to the solvent molecules can become competitive to further inner-shell solvation of the core ion. The shell effects in these systems, if they do occur, are therefore rather diffuse. In such systems it is possible that the outer shells start to form before an inner shell is completed. Moreover, it is also possible that, if the energies are close, a cluster with a completed inner shell is present in equilibrium with isomers where the ligand molecules partially fill inner and outer shells. We shall consider the possibility of the coexistence of isomeric clusters and present a numerical analysis of the effects on the measurement of thermochemical data.

Experimental Section

Measurements were done with the NBS pulsed high-pressure mass spectrometer, which was described elsewhere.[13] For the hydration of H_3O^+ and NH_4^+, the carrier gas was methane at pressures of 1–3 Torr, water was 0.1–20% of the total gas mixture and ammonia was added in trace amounts. For the hydration of OH^-, 0.1–20% water was used in N_2O or a 1/1 mixture of CH_4 and N_2O. For the highest hydration steps in all systems ($n > 5$), the studies were in neat H_2O in the positive ion systems and about 5% N_2O in water in the negative ion system.

In the negative ion systems, the Cl^- ion is always present. This ion and its hydrates can cause mass coincidence with $OH^-·H_2O$ and its hydrates. Therefore, for these studies D_2O was used. D_2O and H_2O were used also in several steps of the $H_3O^+·nH_2O$ system. The results showed no measurable difference between the clustering thermochemistry in light and heavy water systems within the usual error of ±1 kcal/mol and ±2 cal/(mol K). Also, the equilibrium constants were verified to be independent of total pressure and of the partial pressure of water within a factor of 3 in the ranges quoted.

Results and Discussion

A. Sample Clustering Systems. 1. Hydration of H_3O^+. The sample clustering systems in these sections will demonstrate the thermochemical evidence concerning shell filling and the uncertainties in this data.

In cluster **1** the filling of the first shell is expected at $n = 3$. An early series for the $H_3O^+·nH_2O$ system, for $n = 1$–7, was

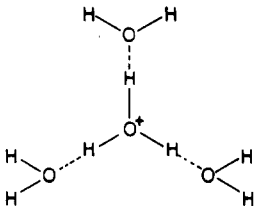

1

obtained by Kebarle et al.[14] in 1967 using pulsed high-pressure mass spectrometry (PHPMS). The enthalpy sequence (i.e., plots of $-\Delta H°_{n-1,n}$ vs. n) did not show a significant break after $n = 3$. However, subsequently Sunner and Kebarle[15] found that the thermal and collisional dissociation of clusters outside the ion source can give erroneously large ΔH and ΔS values under the earlier conditions, especially for the higher clustering steps. Subsequently, the steps $n = 1$–3 were reexamined in Kebarle's laboratory[16] and later also the steps $n = 3$–6.[17] The combined enthalpy sequence from these later studies shows a significant discontinuity after $n = 3$.

The steps $n = 1$–5 were also measured by Beggs and Field[18] using continuous ionization HPMS. Later pulsed measurements on the same apparatus[19] showed that the first two steps in the continuous ionization measurements were probably not in equilibrium and gave erroneous results, while for $n = 3$, and probably for higher n, the clusters were probably in equilibrium. However, a combined series for $n = 1$–2 from the pulsed experiments and $n = 2$–5 from the continuous ionization experiments still does not show a break after $n = 3$.

(4) Dzidic, I.; Kebarle, P. *J. Phys. Chem.* **1970**, *74*, 1466.
(5) Payzant, J. D.; Cunningham, A. J.; Kebarle, P. *Can. J. Chem.* **1973**, *51*, 3242.
(6) Grimsrud, E.; Kebarle, P. *J. Am. Chem. Soc.* **1973**, *95*, 7939.
(7) Hiraoka, K.; Grimsrud, E.; Kebarle, P. *J. Am. Chem. Soc.* **1974**, *96*, 3359.
(8) Hiraoka, K.; Kebarle, P. *J. Am. Chem. Soc.* **1975**, *97*, 4179.
(9) Lau, Y. K.; Kebarle, P. *Can. J. Chem.* **1981**, *59*, 151.
(10) Tang, I. N.; Castleman, A. W. *J. Chem. Phys.* **1972**, *57*, 3638.
(11) Castleman, A. W.; Holland, P. M.; Lindsay, D. M.; Peterson, K. I. *J. Am. Chem. Soc.* **1978**, *100*, 6039.
(12) Castleman, A. W. *Chem. Phys. Lett.* **1978**, *53*, 560.
(13) Meot-Ner (Mautner), M.; Sieck, L. W. *J. Am. Chem. Soc.* **1983**, *105*, 2956.
(14) Kebarle, P.; Searles, S. K.; Zolla, A.; Scarborough, J.; Arshadi, M. *J. Am. Chem. Soc.* **1967**, *89*, 6393.
(15) Sunner, J.; Kebarle, P. *J. Phys. Chem.* **1981**, *85*, 327.
(16) Cunningham, A. J.; Payzant, J. D.; Kebarle, P. *J. Am. Chem. Soc.* **1972**, *94*, 7267.
(17) Lau, Y. K.; Ikuta, S.; Kebarle, P. *J. Am. Chem. Soc.* **1982**, *104*, 1462.
(18) Beggs, D. P.; Field, F. H. *J. Am. Chem. Soc.* **1971**, *93*, 1567.
(19) Meot-Ner (Mautner), M.; Field, F. H. *J. Am. Chem. Soc.* **1977**, *99*, 998.

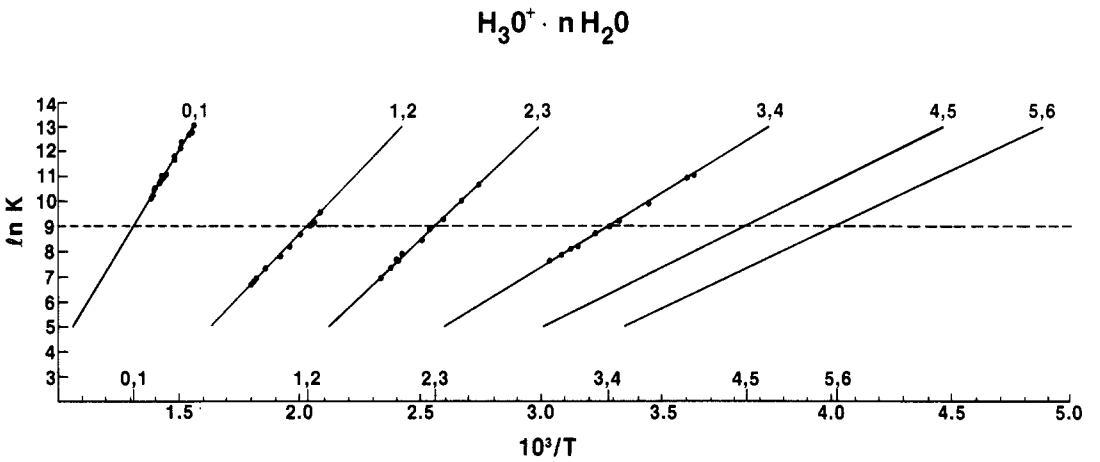

Figure 1. van't Hoff plots for the $H_3O^+ \cdot nH_2O$ system. Least-squares plots are extended between ln K = 5 and 13. Data points from this work; lines for 4,5 and 5,6 equilibria based on data from ref 17. Marks on abscissa show $10^3/T$ values for ln K = 9 for the $n - 1,n$ equilibria. Note the gap in the spacing between the 2,3 and 3,4 plots.

TABLE I: Thermochemical Data for Clustering Reactions[a,b]

cluster	$n-1,n$ 0,1	1,2	2,3	3,4	4,5	5,6	6,7	7,8	ref
					$-\Delta H°$				
$H_3O^+ \cdot nH_2O$	31.8	19.0	17.6	11.5	11.1				this work
	31.6	19.5	17.5	12.7	11.6	10.7			16, 17[c]
	33	21	16.8	12.9	8.5				18, 19[d]
$OH^- \cdot nH_2O$	26.5	17.6	16.2	12.0	11.5	11.2	10.4	(9.8)[e]	this work
	25.0	17.9	15.1	14.2	14.1				20, 21[f]
$NH_4^+ \cdot nH_2O$	20.6	17.4	13.7						this work
	19.9		12.2	10.8	10.6	(9.1)	(8.4)		30
	17.3	14.7	13.4	12.2	9.7				24
$NH_4^+ \cdot nNH_3$	24.8	15.7	13.8	12.5					24
	27	17	16.5	14.5	7.5				25
	25.4	17.3	14.2	11.8					26
		16.9	15.1	13.5	9.6				27
	21.5	16.2	13.5	11.7	7.0	6.5			28
	24.7	16.6	14.6	12.8	8.0				24–28[g]
$NH_4^+ \cdot nHCN$	21.9	17.4	13.7	11.0	7.9				31
					$-\Delta S°$				
$H_3O^+ \cdot nH_2O$	24.0	20.9	27.1	19.9	22.2				this work
	24.3	21.7	27.3	23.4	25.0	26.1			16, 17[c]
	34	20	28	28	17				18, 19[d]
$OH^- \cdot nH_2O$	21.8	21.4	24.1	21.1	24.1	23.2	23.9	(24)	this work
	20.8	21.2	24.8	29.5	33.2				20, 21[f]
$NH_4^+ \cdot nH_2O$	24.6	28.6	24.8						this work
	23.1		21.2	23.0	27.0	(21)	(23)		30
	19.7	21.9	25.1	27.3	22.4				24
$NH_4^+ \cdot nNH_3$	25.9	22.9	25.7	29.4					24
	32	26.8	34	36					25
	24.3	23.9	25.3	27.1					26
		24.8	29.7	31.6	32				27
	20	23.7	25.2	27.9	21.5	21.9			28
	25.6	24.4	26.5	29.4	23.2				24–28[g]
$NH_4^+ \cdot nHCN$	23.4	23.4	21.5	20.9	18.9				31

[a] $\Delta H°$ in kcal/mol; $\Delta S°$ in cal/(mol K). [b] $\Delta S°$ values in parentheses are estimated. [c] Data in this row are best values by Kebarle et al.: for n = 1–3 from ref 16 and n = 4–6 from ref 17. [d] Data in this row from Field et al.: for n = 1 and 2 from ref 19 and for n = 3–5 from ref 18. [e] Calculated from $\Delta G°$ (245) = −3.9 kcal/mol, assuming $\Delta S°$ = −24 cal/(mol K). [f] Data in this row from Kebarle et al.: for n = 1 and 2 from ref 21 and for n = 3–5 from ref 20. [g] Data in this row are average values from ref 24–28.

Because of the ambiguous status of this important clustering system, we measured it again on the NBS mass spectrometer, using the pulsed method throughout. In the present studies the total pressures and the partial pressures of H_2O were lower than in preceding studies. This allowed obtaining van't Hoff plots at somewhat lower temperature ranges than in preceding studies, minimizing thermal ion decomposition outside the source. The experimental results and the van't Hoff plots are shown in Figure 1. The results, in Table I, are in excellent agreement with Kebarle's "best series" of results.

The spacing of the van't Hoff plots from the present results shows a distinct gap after n = 3. The enthalpy sequence (Figure 2) also shows a distinct drop after n = 3. However, we also show in Figure 2 error bars of ±1 kcal/mol. An error of this magnitude is usually associated with the $\Delta H°_{n-1,n}$ values on the basis of the standard deviation of the slopes of van't Hoff plots and the precision of replicate measurements from one or several laboratories. We note that adding 1 kcal/mol to $-\Delta H°_{1,2}$ and $-\Delta H°_{3,4}$ and subtracting 1 kcal/mol from $-\Delta H°_{2,3}$ would eliminate the discontinuity after n = 3. Therefore, while the shell effect may be real, it is within the experimental error limits.

The shell effect is also observed in the entropy sequence (Table I). In ion **1** the ligand molecules apparently hinder each other's rotation, leading to a large negative $\Delta S°$ value of −27 cal/(mol K). The next water molecule in the second shell is not hindered, however, and $\Delta S°$ is less negative, −23 cal/(mol K). However,

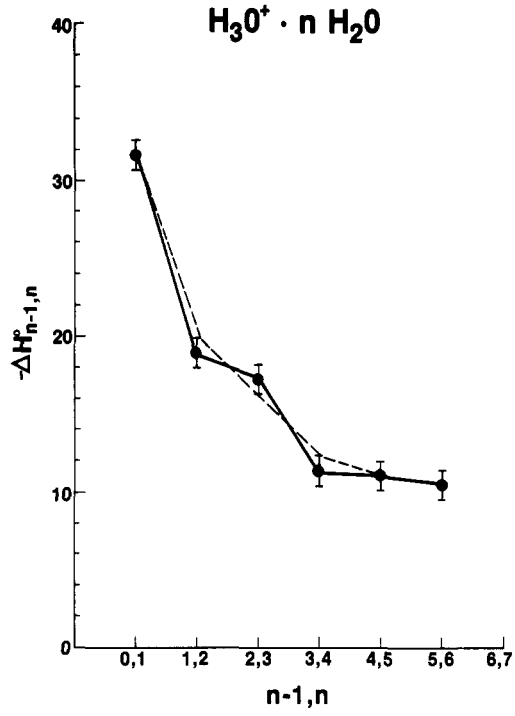

Figure 2. Enthalpy sequence for the $H_3O^+ \cdot nH_2O$ system. Data for n = 1–4 from this work and n = 5 and 6 from ref 17. Broken line through extreme points of the error bars eliminates the break after n = 3.

the effect is again within the combined error of the ±2 cal/(mol K) error for each step.

2. Hydration of OH^-. A series for n = 1–5 was measured by Arshadi and Kebarle using the continuous ionization method,[20] and steps n = 1 and 2 were repeated by the pulsed method,[21] yielding somewhat larger ΔH° values. Again, these measurements were done in neat H_2O. For measurements of n = 3–5, which were done only in the continuous ionization mode, the attachment energies $-\Delta H^\circ_{n-1,n}$ leveled off at about 14 kcal/mol. This is higher than the usual limit of attachment energies for large hydrated clusters, which is usually about the condensation energy of neutral water, i.e., about 10 kcal/mol. The high limiting value suggests an artifact such as thermal ion dissociation in these early studies.

We measured the $OH^- \cdot nH_2O$ series with pulsed ionization, with relatively low concentrations of water, i.e., 1–10% D_2O in a carrier gas. Again, this allows measurements at relatively low temperatures, minimizing thermal dissociation.

Surprisingly, the spacing of the van't Hoff plots (Figure 3) and the enthalpy sequence (Figure 4) show a definite shell effect at n = 3. Unlike in $H_3O^+ \cdot 3H_2O$ (ion **1**), the reason for shell filling in $OH^- \cdot 3H_2O$ is not immediately obvious. There may be two structures that could explain this unexpected behavior. The oxygen in OH^- has three equivalent lone pairs. The hydrogen bonding of one H_2O molecule to each lone pair would complete a first shell (ion **2**), and the fourth water molecule would have to start the second shell. Indeed, Newton and Ehrenberg showed[22] that the branched structure **2** is the most stable isomer of $OH^- \cdot 3H_2O$.

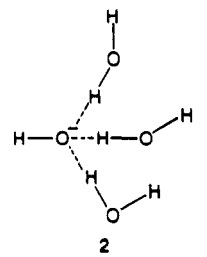

2

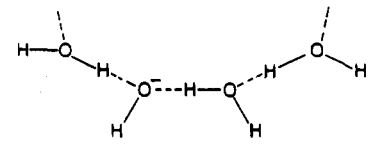

3

(20) Arshadi, M.; Kebarle, P. *J. Phys. Chem.* **1970**, *74*, 1463.
(21) Payzant, J. D.; Yamdagni, P.; Kebarle, P. *Can. J. Chem.* **1971**, *49*, 3308.
(22) Newton, M. D.; Ehrenson, S. J. *J. Am. Chem. Soc.* **1971**, *93*, 4971.

However, it is worth noting that the linear isomer **3** can also explain shell filling at n = 3. In this cluster the first two OH^- units complete the first shell about a symmetric central proton and the next two water molecules complete the second shell. The fourth molecule then starts a new, third linear shell. The linear two-molecule shells in structure **3** are similar to the linear structure that was postulated[23a] and theoretically calculated[23b] for the clusters $(HCN)_nH^+$.

3. Ammoniation and Hydration of NH_4^+. We shall examine next the solvation of NH_4^+ by NH_3. This system has been measured in several laboratories[24-28] and all sets of data show the same trend, which is illustrated by the composite average results in Figure 5. A clear discontinuity is observed between the 3,4 and 4,5 equilibria, consistent with the filling of four inner-shell hydrogen bonds to NH_4^+ before the addition of the fifth NH_3 molecule. Similarly, a discontinuity is also observed in $-\Delta S^\circ_{n-1,n}$, with the entropy becoming less negative at the start of a new, uncrowded shell.

While this system shows a distinct shell effect in Figure 5, even here the magnitude of the effect is just comparable to the experimental error. Moving the $\Delta H^\circ_{n,n-1}$ values corresponding to the 2,3, 3,4, and 4,5 equilibria by 1 kcal/mol eliminates the discontinuity in the plot. Nevertheless, since the data from several sources are all consistent, the probability of error is reduced and the evidence for the filling of the inner shell in the ammoniation of NH_4^+ can be probably accepted. As we shall see below, this is also consistent with some more quantitative criteria. The following paper[29] will show that this is also consistent with ab initio results.

In contrast to ammoniation, the trend in the hydration of NH_4^+ is more ambiguous. The first set of data on this system, by Payzant et al.,[24] shows a small discontinuity after n = 4 (Figure 6). However, changing one data point, $-\Delta H^\circ_{3,4}$ by 1 kcal/mol, from 12.2 to 11.2 kcal/mol, can eliminate this feature. With respect to the experimental data, Sunner and Kebarle[15] showed that in the hydration of K^+ ion decomposition outside the source can cause a significant error, especially for the higher hydrates, i.e., for n = 3–5, the region of interest in shell formation. Again, because of the uncertainty in this system, we measured this system in our laboratory, again using relatively low pressures of H_2O and low temperatures, minimizing dissociation problems. Steps 1–7 were measured previously[30] and 1–3 were repeated in the present work (Table I). The van't Hoff plots, Figure 7, show no grouping effects about n = 4 and 5, and the enthalpy sequence also shows no discontinuity. The following paper[29] will show ab initio results that suggest that isomeric $NH_4^+ \cdot nH_2O$ clusters with inner-shell and outer-shell attachment may reach similar energies already for n = 3. Entropy effects may further facilitate the start of outer-shell filling and lead to isomeric clusters being present in equilibrium.

An even smoother decrease of $-\Delta H^\circ_{n,n-1}$, as well as of $-\Delta S^\circ_{n-1,n}$, is observed when the ligand is HCN[31] (Table I). Again, this indicates that the second shell starts to form before the first shell is filled or that isomeric clusters are present. In either case, the conclusion is that at some stage in clustering, an $NH_4^+ \cdots$ NCH···NHC bond becomes similar in strength to an $NH_4^+ \cdots$NCH bond. This is unexpected in that unconventional $CH^{\delta+} \cdots O$ bond are usually weaker than $NH^+ \cdots O$, i.e., n-donor $H^+ \cdots$n-donor bonds. We shall show elsewhere ab initio results[31] that are in accord with these conclusions.

(23) (a) Meot-Ner (Mautner), M. *J. Am. Chem. Soc.* **1978**, *100*, 4694. (b) Hirao, K.; Yamabe, S.; Sano, M. *J. Phys. Chem.* **1982**, *86*, 2626.
(24) Payzant, J. D.; Cunningham, A. J.; Kebarle, P. *Can. J. Chem.* **1973**, *51*, 3242.
(25) Searles, S. K.; Kebarle, P. *J. Phys. Chem.* **1968**, *72*, 742.
(26) Tang, I. N.; Castleman, A. W. *J. Chem. Phys.* **1975**, *62*, 4576.
(27) Long, J. W.; Franklin, J. L., *Int. J. Mass Spectrom. Ion Phys.* **1973**, *12*, 403.
(28) Arshadi, M. P.; Futrell, J. H. *J. Phys. Chem.* **1974**, *78*, 1482.
(29) Deakyne, C. A., following paper in this issue.
(30) Meot-Ner (Mautner), M. *J. Am. Chem. Soc.* **1984**, *106*, 1265.
(31) Speller, C. V.; Meot-Ner, (Mautner), M.; Deakyne, C. A., unpublished results.

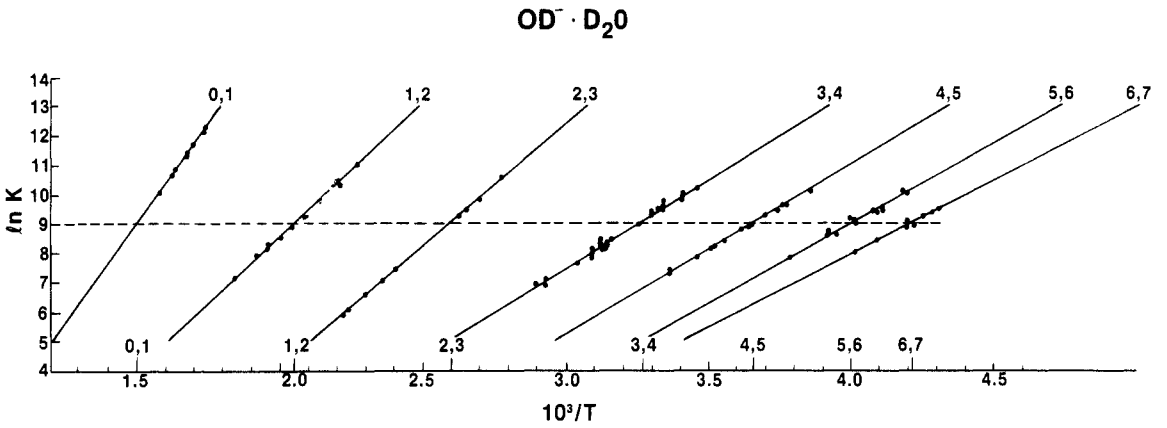

Figure 3. van't Hoff plots for the $OD^-\cdot nD_2O$ systems. Data from this work.

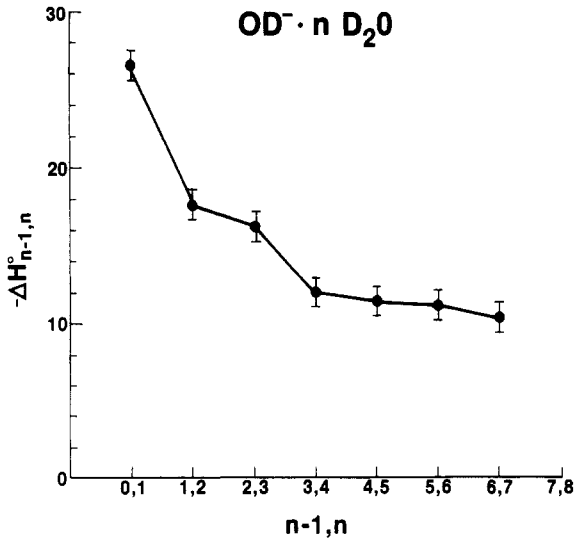

Figure 4. Enthalpy sequence for the $OD^-\cdot nD_2O$ system.

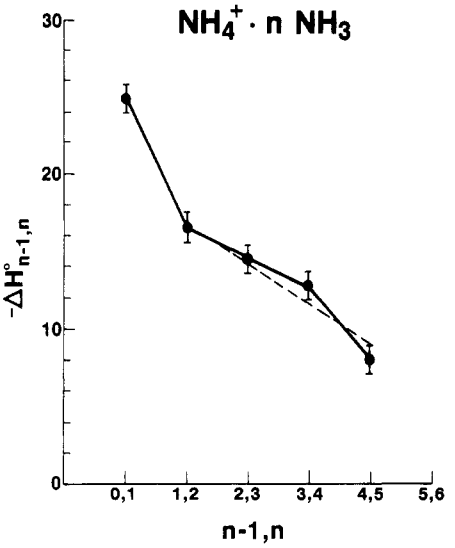

Figure 5. Enthalpy sequence for the $NH_4^+\cdot nNH_3$ system. Average data from four experimental series; see Table I.

B. Thermochemical Criteria for Shell Formation. 1. Discontinuities in Enthalpy Sequences. The criterion applied in the preceding examples to test shell formation may be expressed in a quantitative way. In general, in the absence of structural effects, the charge in the cluster should become more delocalized with each step. The value of $-\Delta H^\circ_{n-1,n}$ steps is expected to decrease with n in the absence of shell effects, and each additional solvent molecule is expected to have a smaller effect on the size of the decrease. Therefore, if no shell is filled at the addition of the sth solvent molecule, then $-\Delta H^\circ_{n-1,n}$ decreases monotonically from $n = s - 1$ to $n = s$ and $n = s + 1$, and eq 3 applies. Conversely,

$$\delta\Delta H^\circ_s = (-\Delta H^\circ_{s-2,s-1}) + (-\Delta H^\circ_{s,s+1}) + 2\Delta H^\circ_{s-1,s} > 0 \quad \text{no shell} \quad (3)$$

$$< 0 \quad \text{shell filled} \quad (4)$$

if a shell is filled by the sth molecule, then the drop in $\Delta H^\circ_{n-1,n}$ after adding the sth molecule will be larger than in going from the $(s - 1)$th to the sth molecule and eq 4 applies.

We apply this criterion in Table II to all the clustering systems of metal and onium ions where the available data extends beyond the expected shell-filling step, i.e., at least to the $(s + 1)$th solvent molecule. In the solvation of metal ions we consider the filling of the first shell or the first four equivalent positions by solvent molecules about the ion. In the case of polyprotonic onium ions we consider the filling of the inner shell by solvent molecules that can hydrogen bond directly to the ion., as, for example, 3 in ion **1**. For monoprotonic onium ions the first shell is filled by the first water molecule (ion **4**) and eq 3 and 4 cannot be applied since

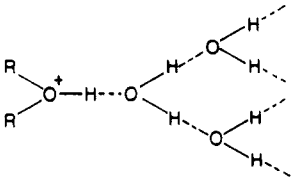

4

$s - 1 = -1$. However, in these cases we consider the filling of the second shell by the third solvent molecule (ion **4**).

Table II shows that in 36 of the 59 values tabulated, $\delta\Delta H^\circ_s$ is negative, which would indicate the distinct filling of shells in

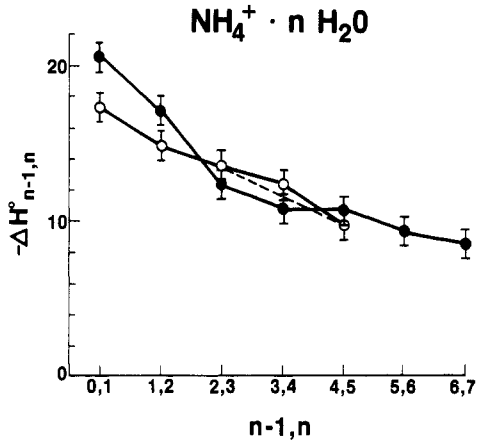

Figure 6. Enthalpy sequence for the $NH_4^+\cdot nH_2O$ system. (●) Data from this laboratory, for n = 1–3 average of this work and ref 30; (○) ref 24. Broken line shows that break after $n = 4$ in the second series of data is eliminated by decreasing $-\Delta H^\circ_{3,4}$ by 1 kcal/mol.

TABLE II: Solvent Shell Formation about Ions

ion	solvent	s^a	$\delta\Delta H°_s{}^b$	$\Delta(10^3/T)_K{}^c$	shell formed[d]	$\delta H°_{s,vap}{}^e$
			Metal Ions, First Shell			
Li^+	H_2O	4	0.8	0.22	N	6
	NH_3	4	−0.9	0.00	?	11
Na^+	H_2O^f	4	0.5	−0.04	?	4
	H_2O^g	4	1.3	−0.03	?	4
	NH_3	4	−1.6	−0.45	Y?	8
K^+	H_2O	4	0.3	0.09	N	1
Rb^+	H_2O	4	0.5	0.04	N	2
	NH_3	4	0.3		N	3
Ag^+	H_2O	4	−1.1	0.21	?	5
	NH_3	4	1.4	0.36	N	7
Bi^+	H_2O	4	0.5	0.01	N	2
Pb^+	H_2O	4	0.6	0.02	N	2
	H_2O	2	0.8	−0.40	?	7
Sr^+	H_2O	4	−0.7	−0.02	Y?	11
	H_2O	2	−0.8	−0.21	Y?	21
			Polyprotonic Onium Ions, First Shell			
NH_4^+	H_2O^h	4	−1.3	0.08	?	3
	H_2O^i	4	1.2	0.13	N	3
	NH_3	4	−2.6	−0.79	Y	5
	HCN	4	0.0	−0.32	?	5
H_3O^+	H_2O	3	−2.8	−0.22	Y	7
H_3S^+	H_2S	3	−1.0	−0.52	Y?	4
$CH_3NH_3^+$	H_2O	3	0.3	0.07	N	1
n-$C_3H_7NH_3^+$	H_2O	3	0.9	0.26	N	0
$(CH_3)_2NH_2^+$	H_2O	2	−0.7	−0.15	Y?	3
$CH_3OH_2^+$	H_2O	2	−2.2	−0.14	Y	11
$CH_3OH_2^+$	CH_3OH	2	−3.4	−0.86	Y	17
$C_2H_5OH_2^+$	H_2O	2	−0.2	−0.14	Y?	9
			Monoprotonic Onium Ions, Second Shell			
H_2COH^+	H_2O	3	−0.8	−0.34	Y?	8
CH_3CHOH^+	H_2O	3	−4.7	−0.85	Y	6
CH_3CNH^+	H_2O	3	−2.5	−0.52	Y	6
$(CH_3)_2OH^+$	H_2O	3	−2.1	−0.23	Y	4
$(CH_3)_2COH^+$	H_2O	3	−1.5	−0.45	Y?	4
$H(NH_2)COH^+$	H_2O	3	0.1	−0.24	?	2
4-CN pyridineH^+	H_2O	3	0.8	0.31	N	0
			Aprotic Solvents, First Shell			
NH_4^+	HCN	4	0.0	−0.32	?	5
Na^+	CH_3CN	3	−1.9	−0.33	Y?	13
K^+	CH_3CN	3	−2.2	−0.31	Y	10
Rb^+	CH_3CN	3	−1.2	−0.24	Y?	8
Cs^+	CH_3CN	3	0.2	−0.22	?	6
NH_4^+	CH_3CN	3	−0.6	−0.08	Y?	13
K^+	$(CH_3)_2SO$	2	−3.0	−0.88	Y	14
K^+	$H_2N(CH_2)_2NH_2$	2	−5.8	−0.50	Y	
H_3^+	H_2	3	−1.1	−4.70	Y?	3
CH_5^+	CH_4	2	−0.3	−1.60	Y?	4
O_2^+	O_2	2	−0.5	−4.70	Y?	5
			$(HCN)_nH^+$ Linear Polymer, Second Shell about the Proton			
$HCNH^+$	HCN	3	−0.6	−0.50	Y?	5
			Hydroxyl Anion, First or Second Shell			
OH^-	H_2O	3	−2.8	−0.30	Y	6
			Negative Ions, First Shell			
OH^-	H_2O	3	−2.6	−0.30	Y	6
CH_3O^-	H_2O	3	0.6	0.02	N	4
CH_3O^-	CH_3OH	3	2.8	0.22	N	6
F^-	H_2O	4	0.2	0.16	N	3
NO_2^-	H_2O	2	−0.3	0.03	?	3
HCO_3^-	H_2O	2	−0.5	0.10	?	4
O_2^-	H_2O	2	−0.6	−0.06	Y?	7
O_2^-	CH_3OH	2	1.6	0.03	N	6
F^-	CH_3CN	4	−3.7	−0.63	Y[j]	2
Cl^-	CH_3CN	3	−2.8	−2.09	Y[j]	3
Br^-	CH_3CN	3	−2.7	−2.38	Y[j]	2
O_2^-	CH_3CN	2	−0.5	0.11	?	6
CO_3^-	H_2O	2	0.0	0.01	N	2

[a] The number of liquid molecules at which shell filling is examined. [b] In kcal/mol. Calculated from eq 4 with the data compiled in ref 2. [c] Calculated with eq 6. $(10^3/T)_{f-1,f}$ is the $10^3/T$ value where ln K = 9 for the given equilibrium, as calculated with $\Delta H°$ and $\Delta S°$ values from ref 2. See also ref 33. [d] Y indicates shell fitted; Y? indicates shell filled tentatively; ? indicates criteria inconsistent; N indicates shell filling not indicated. See text. [e] $\delta H°_{s,vap} = -\Delta H°_{s-1,s} - \Delta H°_{vap}$(solvent). [f] Data of ref 4. [g] Data of ref 35. [h] Data of ref 5. [i] Data of ref 3. [j] Unusually small $S°$ values in the last clustering step (ref 36) suggest an artifact, possibly due to the clustering of neutral CH_3CN at low temperatures.

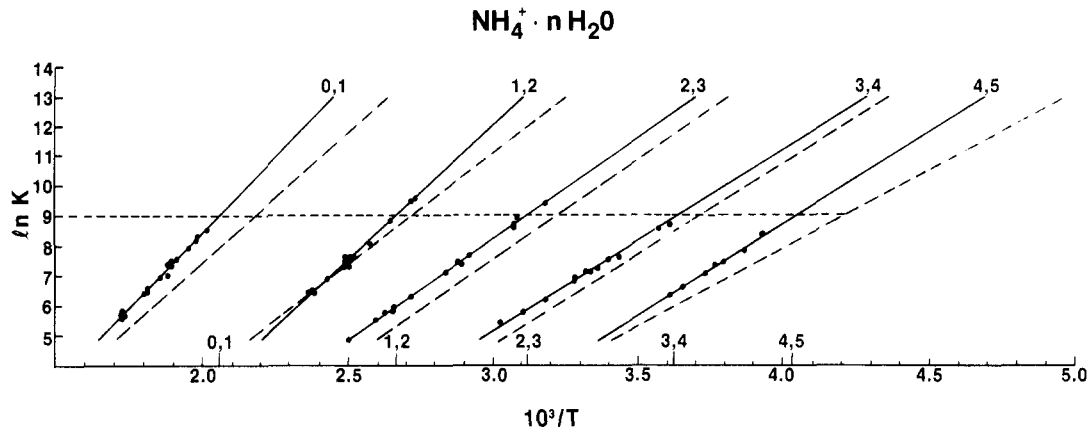

Figure 7. van't Hoff plots for the $NH_4^+ \cdot nH_2O$ equilibria. Points for n = 1–3 from present work and solid lines for n = 4 and 5 from data of ref 30; broken lines, data of ref 24.

these cases. However, it must be remembered that the error associated with each $\Delta H^\circ_{n-1,n}$ measurement is ±1 kcal/mol, and therefore the propagated standard deviation of $\delta\Delta H^\circ_s$ is ±2 kcal/mol. Therefore eq 3 and 4 should be modified to satisfy the criterion considering the experimental error

$$\delta\Delta H^\circ_s > 0 \quad \text{no shell filling}$$
$$0 > \delta\Delta H^\circ_s > -2 \quad \text{shell filling tentative}$$
$$\delta\Delta H^\circ_s < -2 \quad \text{shell filled} \qquad (5)$$

Only 14 of the 59 $\delta\Delta H^\circ_s$ values in Table I satisfy the shell-filling criterion outside this limit.

2. Spacing of van't Hoff Plots. An alternative and more sensitive thermochemical measure of shell formation is the spacing of van't Hoff plots of consecutive clustering steps, as noted in the above examples. Visual inspection of the plots shows the grouping effects in the $H_3O^+ \cdot nH_2O$ and $OH^- \cdot nH_2O$ systems and the absence of a grouping effect in the $NH_4^+ \cdot nH_2O$ system. Tests of this kind were applied qualitatively by Kebarle in some cases, such as in reference to $K^+ \cdot nCH_3CN$.[32]

This test is based on ln K or $\Delta G^\circ_{n-1,n}$ values and it is therefore more sensitive than the previous test that is based on $\Delta H^\circ_{n-1,n}$ values. To illustrate this point, we assume a typical van't Hoff plot between $10^3/T$ = 2.5 and 3.0 and ln K = 5.0 and 8.75, respectively (i.e., $\Delta H^\circ_{n-1,n}$ = −15 kcal/mol). An error of 30% in K at the high temperature, such as may be caused by ion dissociation, would cause an error of 1 kcal/mol in ΔH° but only an error of 0.2 kcal/mol in ΔG°. Since the shell effects that we are examining are on the range of a few kcal/mol, the effect/error ratio is about unity for the ΔH° criterion but an order of magnitude better for criterion based on ΔG° or ln K. This point is illustrated by Figure 7, which shows relatively large differences between the slopes of van't Hoff plots from two sources, while the spacing of the van't Hoff plots from the two sources are in better agreement.

The spacing of the van't Hoff plots can be measured in terms of the $10^3/T$ values required to reach a given value of ln K for each solvation step. In the absence of shell effects the spacing will decrease monotonically. However, if a shell is filled by the sth molecule, a larger drop in the temperature may be needed to start the next, looser shell and there will be a gap in the spacing of the plots. In analogy with eq 3 and 4, eq 6 and 7 are obtained,

$$\Delta(10^3/T)_s = -[(10^3/T)_{s-2,s-1} + (10^3/T)_{s,s+1}] + 2(10^3/T)_{s-1,s} > 0 \quad \text{no shell} \qquad (6)$$
$$< 0 \quad \text{shell filled} \qquad (7)$$

where $(10^3/T)_{n-1,n}$ indicates the temperature at which ln $K_{n-1,n} = c$, where c is a selected constant value. For the present purposes we use c = 9.0, corresponding to equilibrium conditions where P_L = 0.09 Torr and $(BH^+ \cdot nL)/(BH^+ \cdot (n-1)L)$ = 1. These are typical experimental conditions, and indeed most of the data on which Table II is based include points where ln K is near this value. In fact, we obtain the $10^3/T$ value from the published values of ΔH° and ΔS° values. However, this does not increase the error in the calculated values of $10^3/T$ because of compensating errors in ΔH° and ΔS°. The calculated $10^3/T$ values are therefore still based on the more accurate ΔG° values.[33]

Before discussing the results of this criterion, we must note that it is made somewhat ambiguous by the fact that shell formation affects $\Delta S^\circ_{n-1,n}$ as well as $\Delta H^\circ_{n-1,n}$. Therefore shell effects on the spacing of van't Hoff plots can be obscured by compensating enthalpy and entropy effects. For this reason it is preferable to use values of $10^3/T$ at a high value of ln K, i.e., to apply the test at the lowest experimental temperatures included in the van't Hoff plots, where the enthalpy terms predominate.

The above reservation notwithstanding, we note in Table II that the $\Delta(10^3/T)_s$ criterion gives results consistent with the $\delta\Delta H^\circ_s$ criterion in all the cases where the latter is outside the 2 kcal/mol error limit. For these systems, denoted by Y in Table II, the evidence for distinct shell formation can be considered satisfactory.

For 16 further systems both criteria indicate shell filling, but the ΔH°_s criterion is within the 2 kcal/mol error limit. These systems are denoted by Y?. For the other clustering systems the two criteria are inconsistent (denoted by ?) or both indicate the lack of distinct shell formation, denoted by N.

When shell filling about hydrogen bonding onium ions is indicated by our criteria, this occurs at the expected values of s both in the filling of first and second shells. However, in some cases where $-\Delta H^\circ_{s-1,s}$ is small, shell-filling at the expected values of s does not occur, as will be discussed in the next section.

The solvation of metal ions shows some unexpected results. Thus no clear shell effects occur at the expected "solvation numbers" with protic solvent, except possibly in $Na^+ \cdot 4H_2O$. On the other hand, shell-like effects occur at unexpected solvation numbers. For example, $Pb^+ \cdot 2H_2O$ and $Sr^+ \cdot 2H_2O$ may be stabilized by covalent bonds, which are strong only for the first two solvent molecules.[10-12] Also unexpected is the apparent shell effect at n = 3 in $M^+ \cdot nCH_3CN$, which seems to occur with all the alkali metal ions. This may be due to steric effects of the methyl groups that exclude the fourth solvent molecule from the first shell. Similarly, the more bulky $(CH_3)_2SO$ molecule causes a shell-filling effect about K^+ already at n = 2. An interesting effect also occurs in $K^+ \cdot 2NH_2CH_2CH_2NH_2$, where the four ligand NH_2 groups may fill the inner shell, forcing the third bidentate ligand molecule to the second shell.

(32) Sunner, J.; Kebarle, P. *J. Am. Chem. Soc.* **1984**, *106*, 6135.

(33) The $10^3/T$ values at ln K = 9 in Table II are actually obtained from the published ΔH° and ΔS° values. However, errors in ΔH°, as obtained from the slopes of van't Hoff plots, do not affect the calculated $10^3/T$ values, since a compensating error occurs in ΔS° which is calculated from $\Delta S^\circ = (\Delta H^\circ - \Delta G^\circ)/T$. The errors in ΔH° and ΔS° cancel out when ΔG° is reconstructed from ΔG° and $\Delta H^\circ - T\Delta S^\circ$, and this is used to obtain 10^3 at a given ln K.

Finally, special stabilizing effects are indicated by our criteria for $CH_5^+ \cdot 2CH_4$,[34] for $H_3^+ \cdot 3H_2$,[19] and for $HCNH^+ \cdot 3HCN$.[22] The structural reasons for these effects were discussed in the respective papers.

3. Relation of Shell Filling to Condensation Energies. The attachment of several solvent molecules increasingly delocalizes the charge from the core ion BH^+. The crowding of solvent molecules about the ion also results in the mutual repulsion of the solvent molecules. As a result, the thermochemistry for inner-sphere solvation becomes less favorable as the cluster grows. On the other hand, solvent attachment to outer shells involves solvent–solvent interactions, whose limiting value as the cluster increasingly resembles a neutral liquid droplet is $-\Delta H^\circ_{condens}$ of the liquid solvent. (In fact, the lower limit may be somewhat smaller than this value due to surface effects.) It should also be noted that entropy effects usually favor attachment to uncrowded positions in partially empty outer shells vs. the filling of crowded inner shells.

As a result, the filling of the inner shell is expected to be preferred only if the enthalpy of the shell-filling step is significantly more negative than the heat of condensation of the liquid ligand, eq 8. Here the 3 kcal/mol value is an empirical parameter as will be seen presently.

$$-\delta\Delta H^\circ_{s,vap} = -(\Delta H^\circ_{s-1,s} - \Delta H^\circ_{vap}) > 3 \text{ kcal/mol} \quad (8)$$

An example of the relation between $\Delta H^\circ_{s-1,s}$ and $\delta\Delta H^\circ_{vap}$ is provided by comparing the $H_3O^+ \cdot nH_2O$, the $NH_4^+ \cdot nNH_3$, and the $NH_4^+ \cdot nH_2O$ systems. In the first, $\Delta H^\circ_{s-1,s} = 17.5$ kcal/mol, which allows a large drop toward the limiting condensation energy of 10.5 kcal/mol. In the second system, $\Delta H^\circ_{s-1,s} = 12.8$ kcal/mol, which still allows a further significant drop because of the low heat of condensation of the solvent ammonia, 7 kcal/mol. In contrast, for $NH_4^+ \cdot nH_2O$, $-\Delta H^\circ_{s-1,s}$ ($s = 4$) = 10.8 kcal/mol. This is already similar to the heat of condensation of water (and the measured value may in fact correspond to water–water condensation in the outer shell), and, evidently, a large distinguishable decrease in $\Delta H^\circ_{n-1,n}$ in the next step is not possible.

We can examine the applicability of these arguments throughout Table II. The last column shows that in all the cases where solvent shells are clearly filled, $\delta\Delta H^\circ_{s,vap} > 3$ kcal/mol. Conversely, for all cases where $\delta\Delta H^\circ_{s,vap} < 3$ kcal/mol, the data indicate no distinct filling of a solvent shell. However, we note that in some cases, although a large value of $\delta\Delta H^\circ_{s,vap}$ would allow shell filling, this does not seem to occur. Apparently, there may be other factors that prevent shell filling even when this condition is satisfied.

The above observations may be summarized by the following empirical rule:

A necessary but not sufficient condition for the distinct filling of a solvent shell by the sth solvent molecule is that $-\Delta H^\circ_{s-1,s}$ exceeds the condensation enthalpy of the solvent by at least 3 kcal/mol.

Before proceeding further, we wish to point out a physical implication of the lower limiting values observed in enthalpies of clustering. This lower limiting value, observed in 27 hydration systems of metal ions and protonated species in Table II, is 9 ± 1 kcal/mol, which is close to the condensation enthalpy of water. This finding may be interpreted to indicate that the cluster approaches liquidlike behavior. However, it must be remembered that $\Delta H^\circ_{condens}$ of water corresponds to the net formation of two hydrogen bonds. With the assumption that the ionic charge is diffuse in the large clusters where $-\Delta H^\circ_{n-1,n} \cong 10$ kcal/mol, this limiting value then also implies the net formation of two new hydrogen bonds by the added water molecule. This would imply cyclic structures such as in ions **5** and **6**. Another possibility could be that the apparent lower limiting enthalpies may reflect an experimental artifact in that single-bonded clusters with lower

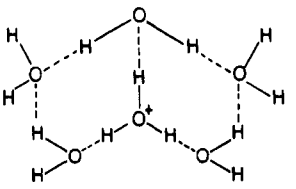

5

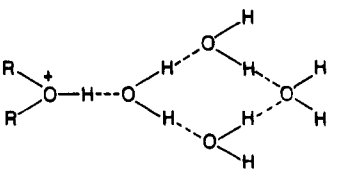

6

attachment lower values cannot be measured, since the measurements would require low temperatures where water condenses in the ion source. However, in several systems the lower value seems to be constant at 10 ± 1 kcal/mol through several solvation steps, indicating that this is a real low limit.

C. Isomeric Clusters and Composite van't Hoff Plots. As we noted above, when $\Delta H^\circ_{s-1,s}$ and $\Delta H^\circ_{condens}$ are close, isomeric clusters with partially filled inner and outer shells may be present at equilibrium in the ion population. We shall now examine the effects of the presence of isomeric ions on the thermochemical measurements.

As an example, we shall assume that ion BH^+ can associate with ligand L to form distinct clusters C_1, C_2, ..., C_i.

$$BH^+ + L \rightleftharpoons C_1^+ \rightleftharpoons C_2^+ \rightleftharpoons C_i^+ \quad (9)$$

When all the reactions are in equilibrium, the measured apparent equilibrium constant is given by

$$K_{app} = (1/P_L)(C_1^+/BH^+ + C_2^+/BH^+ + \ldots + C_i^+/BH^+) \quad (10)$$

$$K_{app} = \sum K_i = \sum(\exp\Delta S^\circ_i/R)(\exp -\Delta H^\circ_i/RT) \quad (11)$$

From (11) and standard equations one obtains for ΔH°_{app} and ΔS°_{app}

$$\Delta H^\circ_{app} = -R \, d \ln K^\circ_{app}/d1/T = \sum(K_i/\sum K_i)\Delta H^\circ_i \quad (12)$$

$$\Delta S^\circ_{app} = (\Delta H^\circ_{app} - \Delta G^\circ_{app})/T \quad (13)$$

where

$$\Delta G^\circ_{app} = -RT \ln K_{app} \quad (14)$$

Equation 12 shows that the apparent value of ΔH° will be weighed toward the clusters whose formation is most exothermic and/or whose population in the equilibrium mixture is largest. In relation to eq 13 it may be noted that the presence of isomeric clusters makes ΔS°_{app} positive. Specifically, if n distinguishable but thermochemically equivalent isomers are present, a conformational entropy of $R \ln n$ results.

To illustrate the effect of isomeric clusters, we use eq 11–13 to calculate ΔH°_{app} and ΔS°_{app} for a precursor ion $BH^+ \cdot (n-1)L$ in equilibrium with two higher clusters $(BH^+ \cdot nL)_1$ and $(BH^+ \cdot nL)_2$. The corresponding thermochemical parameters are denoted ΔH°_1 and ΔH°_2, etc.

The parameters selected for the present example correspond to systems where the formation of isomeric clusters may be significant. For hydration reactions this will occur at relatively large clusters, i.e., n = 3–5, where a large number of structures are possible. The enthalpies of these hydration steps are usually in the range 10–20 kcal/mol.

In the present example we consider $\Delta H^\circ_1 = -15$ kcal/mol and allow ΔH°_2 to vary from −11 to −19 kcal/mol. We also allow a typical value of −23 cal/(mol K) for ΔS°_1 and allow ΔS°_2 to vary from −18 to −28 cal/(mol K). We consider measurements about 400 K and calculate the slopes of the van't Hoff plots and ΔS° obtained from eq 13 at this temperature. The apparent thermochemical results for the apparent reaction 1 are summarized in Table III.

With the parameters used to construct Table III, one or other of the isomers predominates in the upper left-hand and the lower right-hand areas of the table. At these combinations of the

(34) Hiraoka, K.; Kebarle, P. *J. Chem. Phys.* **1978**, *62*, 2267.
(35) Tang, I. N.; Lian, M. S.; Castleman, A. W. *J. Chem. Phys.* **1972**, *57*, 3638.
(36) Yamdagni, R.; Kebarle, P. *J. Am. Chem. Soc.* **1972**, *94*, 2940.

TABLE III: Thermochemical Values in a System with Two Isomeric Cluster Products P_1 and P_2. The True Thermochemical Values for Product P_1 Are $\Delta H°_1$ = −15 kcal/mol and $\Delta S°_1$ = −23 cal/(mol K) and for Product P_1 Are $\Delta H°_2$ and $\Delta S°_2$ as Indicated. The Apparent Thermochemical Values for the Apparent Combined Reaction, as Obtained from the Apparent van't Hoff Plot, Are ($\Delta H°_{app}$; $\Delta S°_{app}$) as Shown.

	$\Delta S°_2$										
$\Delta H°_2$	18	19	20	21	22	23	24	25	26	27	28
19	19.0; 18.0	19.0; 19.0	19.0; 20.0	19.0; 21.0	19.0; 22.0	19.0; 22.9	19.0; 23.9	18.9; 24.8	18.9; 25.7	18.8; 26.4	18.7; 27.1
18	18.0; 18.0	18.0; 19.0	18.0; 20.0	18.0; 20.9	18.0; 21.9	17.9; 22.8	17.9; 23.6	17.8; 24.4	17.7; 25.1	17.6; 25.6	17.3; 25.8
17	17.0; 18.0	17.0; 18.9	17.0; 19.9	16.9; 20.8	16.9; 21.7	16.8; 22.5	16.8; 22.2	16.6; 23.7	16.5; 24.0	16.2; 24.2	16.0; 24.1
16	16.0; 17.9	16.0; 18.8	16.0; 19.7	15.9; 20.6	15.9; 21.3	15.8; 21.9	15.7; 22.4	15.6; 22.8	15.4; 22.9	15.3; 23.0	15.2; 23.1
15	15.0; 17.8	15.0; 18.7	15.0; 19.6	15.0; 20.4	15.0; 21.1	15.0; 21.6	15.0; 22.1	15.0; 22.4	15.0; 22.6	15.0; 22.7	15.2; 22.3
14	14.2; 18.1	14.3; 19.0	14.4; 19.9	14.6; 20.2	14.7; 21.4	14.8; 21.9	14.9; 22.3	14.9; 22.6	14.9; 22.7	15.0; 22.8	15.0; 22.9
13	14.0; 19.1	14.2; 20.2	14.5; 21.0	14.6; 21.7	14.8; 22.2	14.8; 22.5	14.9; 22.7	14.9; 22.8	15.0; 22.9	15.0; 22.9	15.0; 23.0
12	14.3; 20.8	14.6; 21.6	14.7; 22.1	14.8; 22.4	14.9; 32.6	14.9; 22.8	15.0; 22.9	15.0; 22.9	15.0; 23.0	15.0; 23.0	15.0; 23.0
11	14.7; 22.1	14.8; 22.4	14.9; 22.6	14.9; 22.8	15.0; 22.9	15.0; 22.9	15.0; 23.0	15.0; 23.0	15.0; 23.0	15.0; 23.0	15.0; 23.0

TABLE IV: Curvatures of Apparent van't Hoff Plots Produced by the Reactions in Table III, with $\Delta H°_1$ = 15 kcal/mol, $\Delta S°_1$ = −23 cal/(mol K) and $-\Delta H°_2$ and $-\Delta S°_2$ as Shown. The Table Shows $-\Delta H°_{app} = -R[d(\ln K_{app})/(d/T)]$ at 300 and 500 K, i.e., ($-\Delta H°_{app}(300)$; $-\Delta H°_{app}(500)$). The Curvatures of the Apparent Combined van't Hoff Plots Are Reflected by the Difference between $-\Delta H°_{app}(300)$ and $-\Delta H°_{app}(500)$.

	$\Delta S°_2$										
$\Delta H°_2$	18	19	20	21	22	23	24	25	26	27	28
19	19.0; 19.0	19.0; 19.0	19.0; 19.0	19.0; 19.0	19.0; 19.0	19.0; 18.9	19.0; 18.9	19.0; 18.8	19.0; 18.7	19.0; 18.5	18.9; 18.3
18	18.0; 18.0	18.0; 18.0	18.0; 18.0	18.0; 17.9	18.0; 17.9	18.0; 17.9	18.0; 17.8	18.0; 17.6	17.9; 17.5	17.9; 17.2	17.8; 16.9
17	17.0; 17.0	17.0; 17.0	17.0; 17.0	17.0; 16.9	17.0; 16.8	16.9; 16.8	16.9; 16.6	16.8; 16.5	16.7; 16.2	16.6; 16.0	16.4; 15.8
16	16.0; 16.0	16.0; 16.0	16.0; 16.0	15.9; 15.9	15.9; 15.8	15.8; 15.7	15.8; 15.6	15.7; 15.5	15.5; 15.4	15.4; 15.3	15.3; 15.2
15	15.0; 15.0	15.0; 15.0	15.0; 15.0	15.0; 15.0	15.0; 15.0	15.0; 15.0	15.0; 15.0	15.0; 15.0	15.0; 15.0	15.0; 15.0	15.0; 15.0
14	14.3; 14.2	14.4; 14.3	14.5; 14.4	14.7; 14.5	14.8; 14.6	14.8; 14.7	14.9; 14.8	14.9; 14.9	15.0; 14.9	15.0; 15.0	15.0; 15.0
13	14.4; 13.8	14.6; 14.0	14.7; 14.2	14.8; 14.5	14.9; 14.5	14.9; 14.8	15.0; 14.8	15.0; 14.9	15.0; 14.9	15.0; 15.0	15.0; 15.0
12	14.8; 13.9	14.4; 14.2	14.9; 14.5	14.9; 14.6	15.0; 14.8	15.0; 14.8	15.0; 14.9	15.0; 14.9	15.0; 15.0	15.0; 15.0	15.0; 15.0
11	14.9; 14.3	15.0; 14.5	15.0; 14.7	15.0; 14.8	15.0; 14.9	15.0; 14.9	15.0; 15.0	15.0; 15.0	15.0; 15.0	15.0; 15.0	15.0; 15.0

thermochemical values the observed values deviate little from those corresponding to the dominant cluster.

The worst errors in $\Delta H°$ deviate by 1 kcal/mol from either of the true values. This occurs when $\Delta H°_{app}$ = 14 kcal/mol, compared with the true values of 13 and 15 kcal/mol, and when $\Delta H°_{app}$ = 16 kcal/mol compared with the true values of 15 and 17 kcal/mol. With these thermochemical parameters, the concentrations of the two isomers at 400 K are comparable.

The worst error in $\Delta S°$ is 2.2 cal/(mol K). The effect of the conformational entropy is noted when the two clusters are equal, i.e., $\Delta H°_1 = \Delta H°_2$ = −15 kcal/mol and $\Delta S°_1 = \Delta S°_2$ = −23 cal/(mol K), but the measured value is −21.6 cal/(mol K).

To compare these deviations from the true thermochemical values, we note that the error associated with the scatter of points on van't Hoff plots, as obtained from standard deviations of slopes and intercepts, is usually ±1 kcal/mol and ±2 cal/(mol K). These are quite comparable to the present effects due to isomeric clusters. Larger errors can result from artifacts such as cluster dissociation outside the ion source.[15]

The apparent van't Hoff plots are not linear; i.e., the derivative $d \ln K_{app}/(d1/T)$ varies with temperature. Nevertheless, the curvatures are small. Over the temperature range 300–500 K the change in $\Delta H°_{app}$ is always less than 1 kcal/mol. Table IV shows the slopes of the apparent van't Hoff plots of the present study in terms of the $\Delta H°_{app}$ measured at the two extreme temperatures, 300 and 500 K. Again, the difference is observable only at the upper right and lower left portions of Table IV, and even there the change of slope is less than 10%. In no case would a deviation of this magnitude be larger than the usual experimental scatter, and therefore the presence of these isomeric clusters would not be detected.

In summary, the errors resulting from the presence of isomeric clusters are small. This results from the fact that if the difference in the stabilities of the isomers is large one of the isomers will predominate in the equilibrium population and the measured values will correspond to this isomer. On the other hand, if the stabilities of the isomers are similar, the measured value will be close to this common value. The only possible large effect may be a large positive $R \ln n$ entropy effect if a large number of energetically similar but distinguishable isomers are present. Nevertheless, the errors caused by the presence of isomers may be sufficient to obscure the effects of shell filling, which are also in the range of several kcal/mol. Experimentally, the presence of isomeric clusters will not be evident since the resultant curvature of the van't Hoff plots is within the usual error limits.

Registry No. H_3O^+, 13968-08-6; NH_4^+, 14798-03-9; OH^-, 14280-30-9; NH_3, 7664-41-7.